Synthesis and Characterization of a Novel Graft Copolymer Containing Carboxyl Groups and Its Application to Extract Uranium(VI) from Aqueous Media

Thayyath S. Anirudhan, Abdul R. Tharun, Sreenivasan Rijith, Padmajan S. Suchithra

Department of Chemistry, University of Kerala, Kariavattom, Trivandrum 695 581, India

ABSTRACT: A novel poly(methacrylic acid)-grafted-cellulose/bentonite (Cellu-*g*-PMAAc/Bent) superabsorbent composite was prepared through graft copolymerization reaction among cellulose, methacrylic acid, and bentonite in the presence of N,N′-methylenebisacrylamide as a crosslinker and potassium peroxydisulphate as an initiator. The structural and morphological characteristics of the graft copolymer were determined using Fourier transform infrared spectra, scanning electron microscope-energy dispersion analysis, and X-ray diffraction. The effectiveness of the Cellu-*g*-PMAAc/Bent, as adsorbent for the removal and recovery of uranium(VI) from aqueous media, was studied. The effects of pH, contact time, and initial sorbate concentration were studied to optimize the conditions for maximum adsorption. The adsorption process, which was pH dependent, shows maximum removal (>99.0%) at pH 6.0. Kinetic study showed that 180 min of contact at 100 mg/L could adsorb about 99.2% of U(VI) onto Cellu-*g*-PMAAc/Bent. A pseudosecond-order kinetic model successfully described the kinetics of sorption of U(VI). Adsorption equilibrium data were correlated with the Langmuir, Freundlich, and Redlich–Peterson isotherm models. The best fit was obtained with Freundlich model. Desorption of U(UI) was studied by using 0.1*M* HCl. Adsorption/desorption for more than six cycles showed the possibility of repeated use of this graft copolymer for the recovery of U(VI) from aqueous solutions. © 2011 Wiley Periodicals, Inc. J Appl Polym Sci 122: 874–884, 2011

Key words: superabsorbent composite; graft copolymer; cellulose; bentonite; uranium(VI); adsorption

INTRODUCTION

In recent years, considerable research attention has been focused on superabsorbent polymers (SAPs) because of their interesting physical properties and potential applications in biomedical fields and in industries such as actuators, drug delivery, artificial muscles, sensors, and different chemomechanical devices and now in the area of purification process.[1,2] SAPs show various characteristic properties such as flexibility, reversible deformation, pH responsiveness, and large surface area.[3] Natural-based SAPs have attracted much attention in many applications because of their nontoxicity, biocompatibility, and biodegradability. Also, the introduction of hydrophilic groups increases the number of pores that aids in the easy loading of metal ions,[4,5] which is a characteristic property needed for the present work. Two types of monomers were used for the synthesis of SAPs. Hence, SAPs can be called as polymer alloys, which are formed by the permanent entanglement of two types of polymers.

The organic–inorganic superabsorbent composites are regarded as promising materials of great scientific interest because of their relative low productive cost, biocompatibility, excellent absorption properties, and wide applications. Superabsorbent composites may display more properties of the effective adsorbents than inorganic and organic components individually. Cellulose (Cellu) is a well-known adsorbent for metal ions in diluted effluents. The applications of Cellu have been found to be limited because of its solubility in acidic and basic medium. Grafting polymer chains onto the backbone of Cellu has been pointed out as a convenient method for improving physical, chemical, and mechanical properties of Cellu as well as preventing solubility. Sorption properties can be improved by grafting new functional groups onto the Cellu. Among different functional groups, carboxylic acid functional group is important because of the high potential of the carboxylate functionality for the removal of heavy metal ions from aqueous solutions. Clays, particularly montmorillonite (Mont) and bentonite (Bent), are widely used as potential inorganic binding matrices for the preparation of composite materials.

Correspondence to: T. S. Anirudhan (tsani@rediffmail.com).

Bent is a type of clay mainly composed of Mont that is a 2 : 1 type alumino silicate. The incorporation of Bent into the polymer matrix can not only reduce production cost but also improve swelling ability, gel strength, mechanical, and thermal stability of corresponding superabsorbent composite.[6,7] In addition to this, Bent shows affinity to some metals, especially uranyl ions, which are also of special interest in the present study.[8,9]

The recovery of uranium from natural sea water and industry wastewater is a challenging problem for chemists, because uranium is one of the important resources to secure energy. Moreover, based on the fundamental principles of radioactive waste management, uranium waste minimization should be done in an effective manner. Adsorption is an effective and versatile method for the recovery of U(VI) because of its high efficiency, easy loading, availability, reusability, and cost effectiveness. A variety of polymer adsorbents incorporated with efficient functionalities such as carboxylic, amidoxime, hexaketone, dithiocarbamate, phosphero, dihydrooxophosphoric, and sulfonic have been reported for the recovery of U(VI) from aqueous solutions and wastewater. Recent investigation[10] has shown that graft copolymers posses impressive binding capacities or removal efficiencies for the sorption of U(VI) from aqueous solutions. Only few studies on superabsorbent composite based on polysaccharides-grafted-vinyl monomer have been reported so far.[11] It was also reported that organic cation exchangers containing acid groups (sulfonic acid, carboxyl group) are more effective in the removal of U(VI) ions,[12,13] which in fact is a major criteria in the selection of acid group containing polymers. In this work, a novel poly(methacrylic acid)-grafted-cellulose/bentonite (Cellu-g-PMAAc/Bent) superabsorbent composite with polymer network was prepared by graft copolymerization with Cellu, MAAc, and Bent in the presence of N,N'-methylenebisacrylamide (MBA) as crosslinker and potassium peroxydisulphate ($K_2S_2O_8$) as an initiator. The objective of the work is to study the feasibility of using Cellu-g-PMAAc/Bent as an adsorbent for U(VI) recovery from aqueous solutions. The adsorption capability, adsorbent kinetics, isotherm, and reversibility of the adsorbent were investigated in batch experiments.

EXPERIMENTAL

Materials

All chemicals and reagents used for experiments and analysis were of analytical grade and were used without further purification. Bent and Cellu samples were purchased from Fluka Chemie (Buchs, Switzerland).

MAAc (98%), MBA (99%), $K_2S_2O_8$ (98%), and sodium bicarbonate were obtained from E. Merck India. The chemical composition of the Bent estimated by the classical scheme of analysis[14] is 46.3% SiO_2, 15.1% Al_2O_3, 4.4% Fe_2O_3, 16.1% CaO, 1.7% MgO, 0.9% TiO_2, 0.8% Na_2O, 0.6% K_2O, and 13.6% loss of ignition. Sodium dithiocarbamate (99%) was purchased from Sigma-Aldrich (Sigma, St. Louis, MO). A stock solution of 1000 mg/L of U(VI) was prepared by dissolving accurately weighed $UO_2(NO_3)_2 \cdot 6H_2O$, (Fluka, Switzerland) in distilled water. Working solutions were prepared by diluting the stock solution.

Preparation of (Cellu-g-PMAAc/Bent) composite

The adsorbent material, Cellu-g-PMMAc/Bent composite from Cellu, Bent, and MAAc was synthesized according to the following procedure. About 6.0-g MAAc, 1.0-g Cellu, 1.0-g Bent, and 20-mL of water (to dissolve the monomer) were introduced in a 500-mL flask kept at 30°C. After 10-min stirring, 0.15-g MBA, the crosslinker, was added under the nitrogen atmosphere. Then 0.2-g $K_2S_2O_8$ as an initiator was added to the reaction mixture. The polymerization temperature was set at 70°C for 4 h to ensure complete consumption of the monomer. On completion of polymerization reaction, 1.5-g sodium bicarbonate was added that acts as a porogen, which prevents the hardening of the grafted polymer. The grafted polymer composite was then filtered and washed several times with ethanol to remove any unreacted monomers and homopolymers. Washing with ethanol will remove the dissolved homopolymer and water from the surface of the product. The product was then dried in an air oven by keeping the temperature at 50°C for 4 h. The dried sample was ground and sieved to obtain 80 ± 230 mesh size of particles (average diameter of 0.096 mm). The grafting density (D%) of the composite was calculated on the basis of dried weight of Cellu and Bent from the increase of weight of the grafting according to equation:

$$D\% = [(W_g - W_i)/W_g] \times 100, \qquad (1)$$

where W_i is the dry weight of Cellu and Bent, and W_g is the dry weight of composite.

The concentration of the carboxylic acid groups in the graft copolymer was determined by acid–base titration method. The carboxylic acid groups of Cellu-g-PMAAc/Bent were first treated with HCl for the recovery of COOH groups, which might be in basic nature on treatment with Na_2CO_3. Thus, treated composite was then neutralized with a known excess of NaOH($V_{NaOH} \cdot C_{NaOH}$), and their unreacted NaOH was titrated with HCl. The concentration of the carboxylic acid groups was determined

as follows: $[COOH] = V_{NaOH}C_{NaOH} - V_{HCl} \cdot C_{HCl}$, where $V_{HCl} \cdot C_{HCl}$ is the amount of HCl used during titration.

Swelling measurements

A weighed quantity of superabsorbent composite (0.025 g) was put into a weighed tea bag and immersed in 100-mL distilled water and allowed to swell 4 h at room temperature. The equilibrated swollen SAPs were allowed to drain by removing the tea bag from water and hanging until no drop drained ($\sim$ 20 min). The bag was then weighed to determine the weight of the swollen SAP (weight of the swollen tea bags was reduced). The swelling capacity $Q(g/g)$ was calculated by:

$$Q = (M - M_0)/M_0, \qquad (2)$$

where M (g) represents the mass of the swollen hydrogel, and M_0 represents the mass of the dried hydrogel. The effect of swelling on the basis of initiator (MBA) and Bent has been studied.

Adsorption/desorption experiments

Adsorption experiments were carried out in thermostated water bath shaker at 30°C with a shaking speed of 200 rpm using 100 Erlenmayer flasks. Batch experiments were performed by equilibrating 0.05 g of adsorbent with 50-mL U(VI) solutions of predetermined initial concentrations. The initial pH of the solutions was maintained at 6 by adding 0.1M NaOH and HNO$_3$. The suspensions were shaken for 4 h. The solid and the liquid phases were separated by centrifugation at 6000 rpm for 10 min, and the U(VI) concentrations in liquid phase were determined by a simple and sensitive spectrophotometirc method based on a colored complex formed with sodium dithiocarbamate in aqueous medium. The amount of adsorbed U(VI) at equilibrium (q_e) was calculated from the difference between the initial and final concentrations of U(VI) in aqueous phase. All the adsorption experiments were done in duplicate. The difference in results for the duplicates was <4%.

Desorption of U(VI) from the spent adsorbent was studied with an aqueous solution of HCl (0.001–0.1M). The U(VI) loaded Cellu-g-PMAAc/Bent (0.05 g) was placed in the desorption medium and shaken for 4 h at 30°C. After centrifugation, the supernatant was analyzed for U(VI) concentration. The desorption ratio was calculated from the amount of U(VI) adsorbed in the adsorbent and the final metal concentration in the desorption medium.

Measurements

The Fourier transform infrared (FTIR) spectra of the samples were obtained from Perkin–Elmer FTIR-180 (Germany) spectrometer in the wavelength range 400–4000 cm^{-1} using a KBr window at a resolution of 4 cm^{-1}. The surface morphology of the adsorbent, before and after U(VI) loading, was identified by Philips Model XL-30CP (Japan) scanning electron microscope (SEM). The samples for taking SEM images were coated with gold prior to SEM examination. Powder X-ray diffraction (XRD) patterns of the samples were taken in a Rigaku (Geigerflex, Japan) diffractometer using nickel-filtered Cu K$_\alpha$ radiation at a scanning speed of 2° min^{-1} and at a wave length of 1.5406 Å. The pH of the solution was measured with a Systronic Microprocessor pH meter (model μ-362, India). A temperature-controlled water bath flask shaker (Lab line, India) was used for shaking the solutions. The spectrophotometric determination of the concentration of U(VI) in solution was done on a Jasco UV-visible (model V-530, India) spectrophotometer by measuring absorbance at λ_{max} of 662 nm.

RESULTS AND DISCUSSION

Synthesis and characterization of the adsorbent

Graft copolymerization of the MAAc onto the cellulose backbone was carried out in a homogenous system using K$_2$S$_2$O$_8$ as a radical initiator and MBA as a crosslinking agent. A schematic illustration of the preparation of Cellu-g-PMAAc/Bent is shown in Scheme 1. The mechanism involved in the graft copolymerization of MAAc/MBA onto Cellu using the said initiator system has been proposed by earlier workers.[15] This anionic radical abstracts hydrogen from hydroxyl group of the cellulose to form the Cellu macroradicals. In the presence of vinyl monomer, the Cellu macroradical is added to the double bond of the monomer resulting in a covalent bond between the monomer and the Cellu with creation of a free radical on the monomer, i.e., a chain is initiated. The homopolymerization reaction may be favored by the radicals such as H and/or OH formed according to the following reactions:

$$\qquad (3)$$

$$\qquad (4)$$

Since a crosslinking agent (MBA) is present in the system, a polymer network is formed with free COOH groups at the chain length. The Bent particles
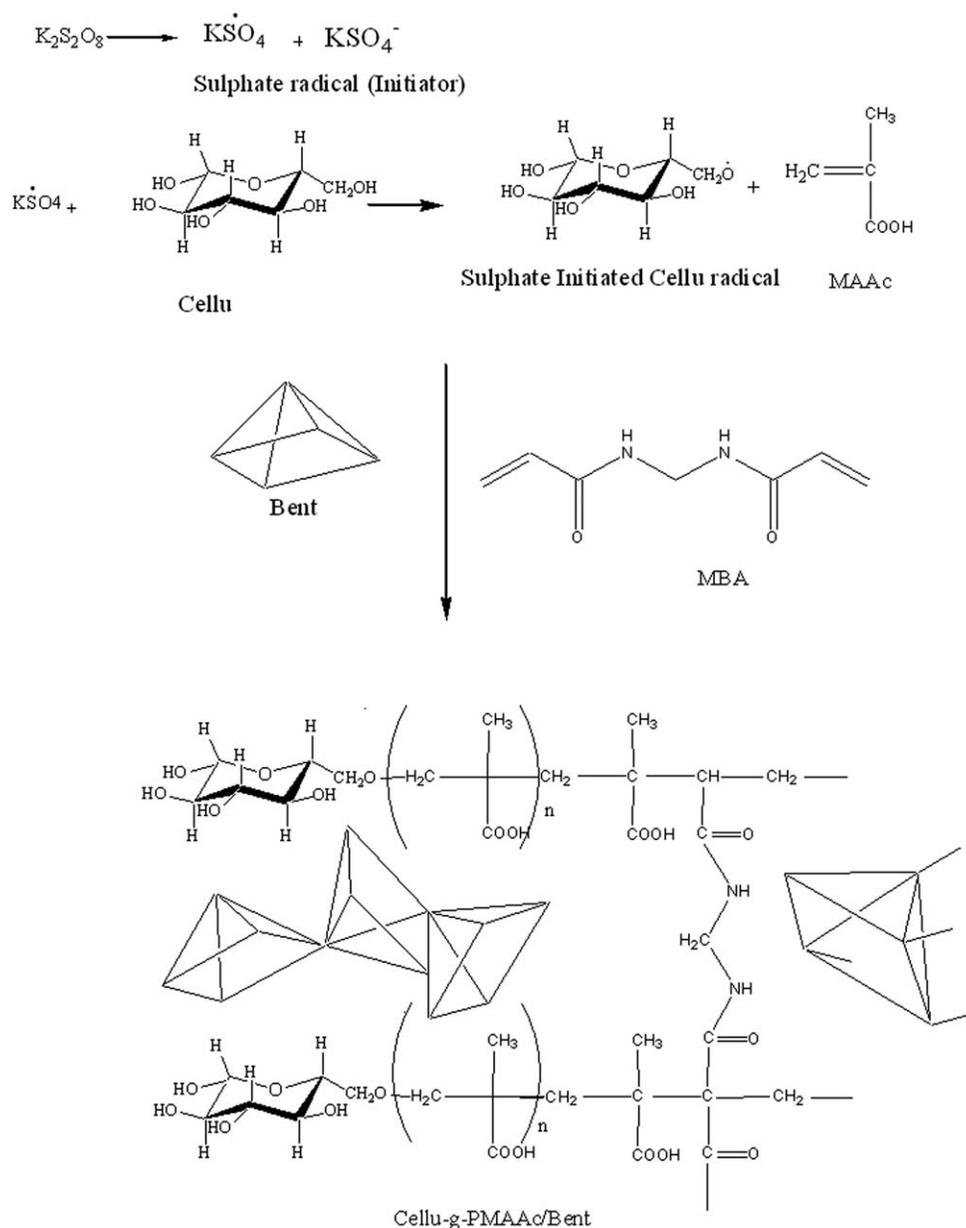
Scheme 1 Preparation of Cellu-*g*-PMAAc/Bent composite.

in the network enhance the swelling ability and mechanical strength. The degree of MAA grafting on the composite was found to be 61.0%, which is much greater than that of the reported values. The amount of carboxylic acid groups in Cellu-*g*-PMAAc/Bent was found to be 1.91 meq/g.

The FTIR spectra of the Cellu, Bent, PMAAc, Cellu-*g*-PMAAc/Bent, and U(VI)-loaded Cellu-*g*-PMAAc/Bent are shown in Figure 1. The absorption band at 3334 cm^{-1} in the spectrum of Cellu corresponds to the hydrogen bonded O—H stretching vibration, and the band at 2900 cm^{-1} represents the C—H stretching of the —CH$_2$ groups from the Cellu. The band at 897 cm^{-1} is characteristic of glucosidic ring in cellulose structure. The band observed

around 3623 cm^{-1} for Bent is assigned to O—H stretching vibration from Mg—OH—Al, Al—OH—Al, and Fe—OH—Al in the octahedral layer. The peaks at 1025 and 814 cm^{-1} are due to asymmetric and symmetric stretching in O—Si—O group. The broad adsorption band observed around 3410 cm^{-1} in the spectrum of PMAAc indicates the presence of $\nu_{O\text{-}H}$ from —COOH group. The PMAAc spectrum exhibits characteristic IR peaks of carboxylic acid groups because of the stretching vibration of C=O (at 1720 cm^{-1}), C—O (at 1270 cm^{-1}), and C—OH (at 1375 cm^{-1}). The absorption peak at 2925 cm^{-1} can be assigned to the in-phase stretching vibration of —CH$_2$ group. The characteristic peaks of Bent observed at 3623, 1025, and 814 cm^{-1} were repeated
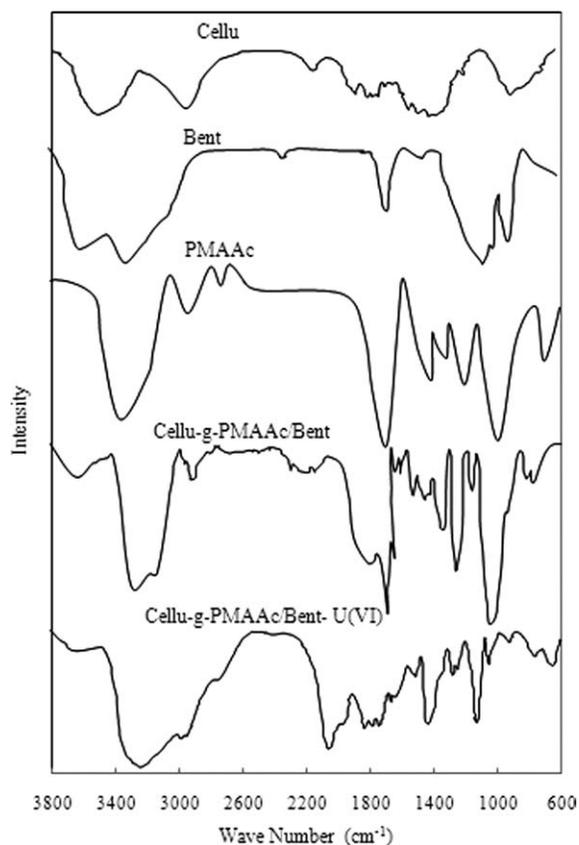
Figure 1 FTIR spectra of Cellu, Bent, Cellu-*g*-PMAAc/ Bent, and U(VI)-loaded Cellu-*g*-PMAAc/Bent.

in the spectrum of Cellu-*g*-PMAAc/Bent composite, indicating that the Bent is incorporated in the polymer network. The spectrum of Cellu-*g*-PMAAc/Bent shows a broad peak centered at 3362 cm^{-1} corresponds to the overlapped band arising from O—H stretching vibrations from carboxyl group and the N—H stretching vibration from the amide groups. A peak appeared at 1650 cm^{-1} because of the carbonyl shielding from the amide group of MBA. The bands at 1640 and 1620 cm^{-1} are due to C=O stretching vibrations (amide shift) and N—H bending vibrations. The characteristic C=O stretching and C—OH in plane bending frequencies of the carboxyl groups observed at 1270 and 1360 cm^{-1}, respectively, in the spectrum of the graft copolymer confirm the grafting of MAAc onto cellulose. A sharp peak at 1720 cm^{-1} observed in the spectrum of Cellu-*g*-PMAAc/Bent further confirms the presence of —COOH moiety. All these characteristic peaks of PMAAc were observed in the spectrum of PMAAc described earlier. New peaks appeared at 1300 and 1420 cm^{-1} in the spectrum of U(VI)-loaded Cellu-*g*-PMAAc/Bent composite, indicating that the —COOH moiety gets converted into its salt—carboxylate.[16,17] This clearly indicates the fact that O=U=O get attached to the COOH moiety by replacing the H$^+$ ion. The band at 918 cm^{-1} corresponds to asymmetric stretching

vibration, v$_a$ (U=O) of the O=U=O group. Also two peaks observed at 698 and 665 cm^{-1}, which are absent in Cellu-*g*-PMAAc/Bent, indicates the presence of U(VI) attachment.[18]

The XRD patterns of Bent, Cellu, Cellu-*g*-PMAAc/ Bent, and U(VI)-loaded Cellu-*g*-PMAAc/Bent are shown in Figure 2. In cellulose XRD pattern, the diffraction maxima at 2θ = 15.0° and 23.5° can be attributed to its crystalline region. These peaks are repeated in the XRD of Cellu-*g*-PMAAc/Bent composites. The peaks in the XRD of Bent at 2.02 and 1.69 Å represent the presence of iron oxide phase as impurity. The XRD pattern of the Bent also indicates the presence of calcite (2.32 and 2.08 Å) and quartz (3.33 Å). The XRD patterns show a *d* (001)-value of 19.1 Å. The characteristic *d* spacing values of Bent is 4.45, 2.54, and 1.49 Å. The peak at 4.45 Å implies the 2 : 1 mineral-type Bent. The XRD patterns of Cellu-*g*-PMAAc/Bent show the characteristic *d*-spacings at 5.96, 4.41, 3.93, and 2.87 Å, indicating the
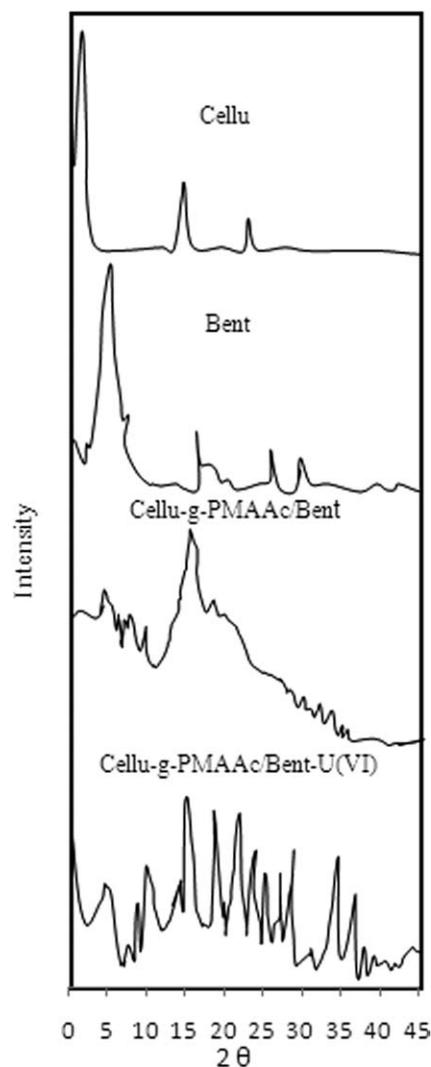

Figure 2 XRD patterns of Cellu, Bent, Cellu-*g*-PMAAc/ Bent, and U(VI)-Cellu-*g*-PMAAc/Bent.
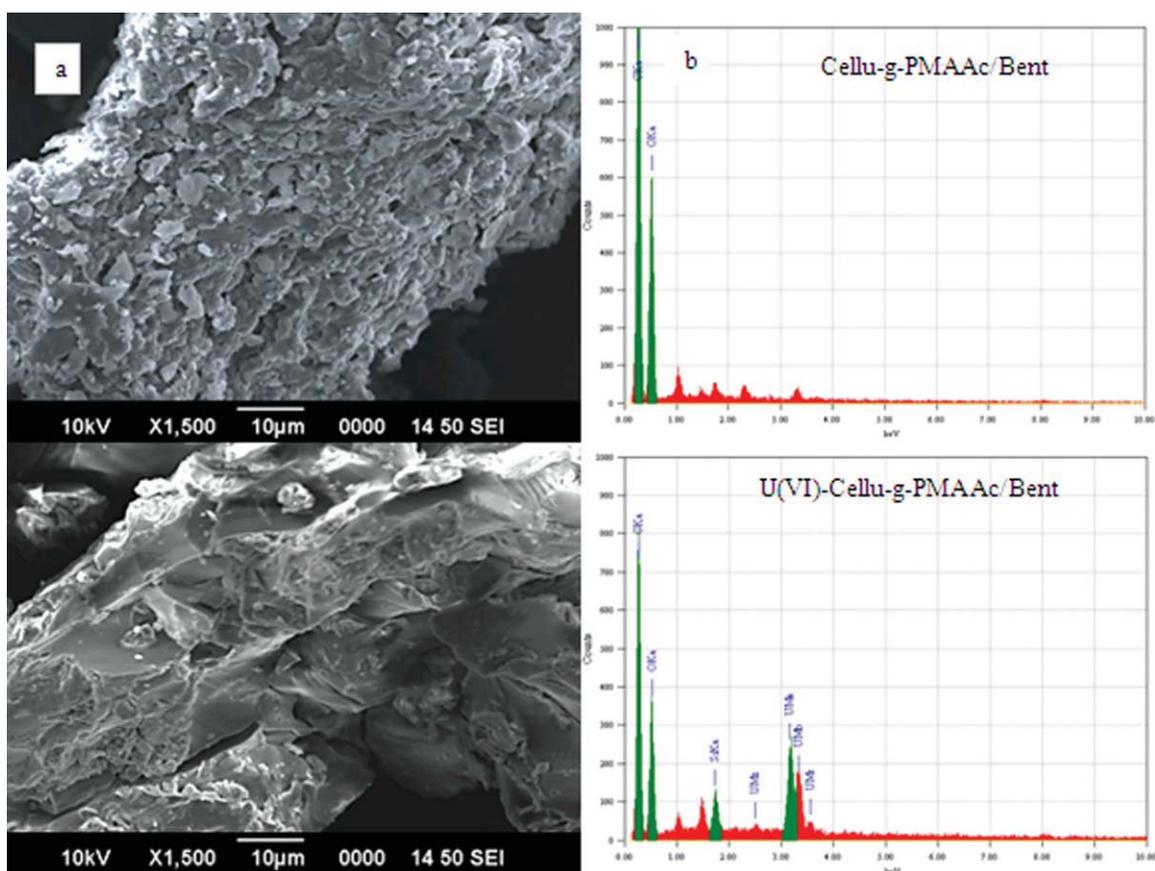
Figure 3 (a) SEM images and (b) EDS spectra of Cellu-*g*-PMAAc/Bent and U(VI)-Cellu-*g*-PMAAc/Bent. [Color figure can be viewed in the online issue, which is available at wileyonlinelibrary.com.]

crystallinity in the polymeric network. The crystalline nature of cellulose and bentonite remains intact even after polymerization process. The XRD patterns show exfoliation nature of the graft copolymer. The implication is that the bentonite is getting exfoliated but not intercalated in the polymer matrix. The 2θ values observed in U(VI)-loaded Cellu-*g*-PMAAc/Bent, 25° and 27°, indicate the presence of U(VI) ions, and it is also confirmed further by the higher 2θ values, i.e., 34° and 38°, which shows its absence, in the pure Cellu-*g*-PMAAc/Bent.[19] These studies clearly indicate that the U(VI) ions get adsorbed onto the Cellu-*g*-PMAAc/Bent.

The SEM images of the Cellu-*g*-PMAAc/Bent and U(VI)-loaded Cellu-*g*-PMAAc/Bent are shown in Figure 3. The micrograph of Cellu-*g*-PMAAc/Bent shows a porous structure. These types of porous structure significantly increase the available surface area of Cellu-*g*-PMAAc/Bent and thus increasing the adsorption capacity. The main part of Cellu-*g*-PMAAc/Bent volume is composed of the interconnected large pores resulting in increase in surface area. It is supposed that these pores have the regions of water permeation and interaction sites with the hydrophilic groups of the graft copolymers. In the case of U(VI)-loaded Cellu-*g*-PMAAc/Bent, the porous nature of the parent compound gets reduced, which means some attachments have enhanced the smooth nature of the composite. It clearly indicates that U(VI) gets adsorbed in Cellu-*g*-PMAAc/Bent composite.

Figure 3 shows the energy dispersion analysis (EDS) of the Cellu-*g*-PMAAc/Bent before and after the U(VI) adsorption. The EDS spectrum of Cellu-*g*-PMAAc/Bent shows the presence of sodium, aluminum, and silicon (0.2, 0.5, and 1.8 keV), indicating the substantial amounts of these metals in the adsorbent. The EDS spectrum of the U(VI)-loaded Cellu-*g*-PMAAc/Bent shows peaks at 2.5, 3.1, 3.2, and 3.5 keV, and this clearly indicates the incorporation of U(VI) onto adsorbent surface.

Effect of bent and the crosslinker MBA content on swelling capacity

The effect of introduced Bent on swelling behavior of Cellu-*g*-PMAAc/Bent was studied in this section. The results show that swelling ability of the composite increase with increase in Bent content incorporated into the composite. The swelling capacity was found to be 910, 1100, 1165, 1216, and 1230 mg/g for 0.4-, 0.6-, 0.8-, 1.0-, and 1.2-g Bent content,

respectively. Bent contains several cations, and they are easily ionized and dispersed into the polymer network, which enhances hydrophilicity of composite and makes it swell more. However, increase in Bent for more than a particular percentage may cause decrease in swelling behavior. Addition of more amount of Bent causes higher crosslink density, which may result in tighter network formation, preventing water to permeate.[20] So the amount of Bent to be added was selected below 10.0 wt %. This observation was according with some other researches where the maximum amount of Bent incorporated in composite was below 10.0 wt %.[21] From these facts, it can be concluded that 1.0-g Bent is enough for its incorporation in the preparation of Cellu-g-PMAAc/Bent composite.

Similarly in the case of MBA, increase in the amount of crosslinker decreases the swelling capacity. The swelling capacity was studied with varying amounts of MBA (0.05, 0.10, 0.15, 0.20, 0.25, 0.30, and 0.35 g) and without Bent. It has been shown that the swelling capacity increased from 930 to 2220 mg/g when the concentration of MBA increased from 0.05 to 0.15 g, thereafter the value decreased to 810 mg/g with the increase of MBA concentration from 0.15 to 0.35 g. More crosslinking concentration causes higher crosslinking density and thus decreasing the space between the copolymer chains and consequently, the resulted highly crosslinked rigid structure cannot be expanded and hold a large quantity of water. Such a well-known behavior was reported earlier.[22,23]

Effect of bent content on thermal stability

The influence of Bent content on thermal stability of Cellu-g-PMAAc/Bent composite was studied, and the results are shown in Figure 4. As can be seen from the figure, all the samples exhibit a three-stage thermal decomposition process. The initial weight loss upto 200°C is due to the moisture loss from the surface of the adsorbent, and it was found to be 16.0, 14.0, 11.0, 10.5, and 9.7% for 0.4, 0.6, 0.8, 1.0, and 1.2-g Bent incorporated in Cellu-g-PMAAc/Bent composite. The second degradation resulting 77.0, 74.0, 68.8, 64.0, and 62.0% weight loss for 0.4, 0.6, 0.8, 1.0, and 1.2-g Bent content, respectively. This loss in weight may be due to the splitting of Cellu structure and chain scission evolving CO, CO_2, and formation of carbonaceous residues and also the intercalated water molecules. Above 500°C, additional 8.0–5.0% weight loss experienced depends on the quantity of Bent content into the Cellu-g-PMAAc/Bent composite.[24] This loss is mainly due to the decomposition of carboxylic groups, dehydration of intercalated moisture, and carbonization of PMAAc chains. Based on the TG analysis, the maxi-
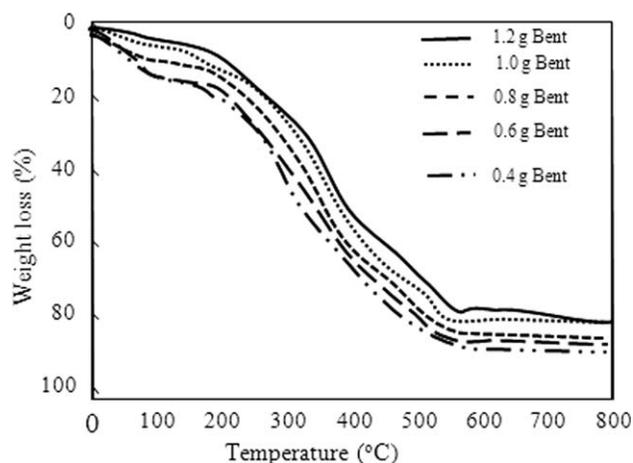

Figure 4 Thermogravimetric analysis of Cellu-g-PMAAc/Bent with the varying amounts of Bent.

mum decomposition temperature of the composite was calculated from the peak of the first derivatives. The maximum decomposition temperature is related to the heat resistivity of the samples. The maximum decomposition temperature was determined to be 332, 340, 348, 353, and 355°C, respectively, for 0.4-, 0.6-, 0.8-, 1.0-, and 1.2-g Bent content incorporated in Cellu-g-PMAAc/Bent composite. As can be expected, the incorporation of Bent caused a significant improvement in thermal stability of the Cellu-g-PMAAc/Bent composite. It may be due to the fact that increase in Bent particle increases the network rigidity and hold down the movement of the adsorbed water embedded in the network. Because of this fact more energy is needed for dehydrating, and hence at higher temperatures, water is getting dehydrated. In addition to that the Bent can act as a heat barrier and thus enhancing the overall thermal stability of the composite.[25]

Effect of pH on U(VI) adsorption

The pH of the aqueous solutions containing the adsorbent is an important parameter in adsorption process. The adsorption of U(VI) onto Cellu-g-PMAAc/Bent as a function of pH is shown in Figure 5. It can be seen that the adsorption of U(VI) onto Cellu-g-PMAAc/Bent has a strong pH-dependent characteristics. For pH from 2.0 to 4.0, the adsorption of U(VI) increased with increase of the pH but appeared to approach a plateau and then no further noticeable increase was observed for pH from 4.0 to 6.0. The increase in U(VI) adsorption is likely related to the pH-dependent charges on the surface functional groups. At low pH, the carboxyl groups on Cellu-g-PMAAc/Bent surface are protonated, resulting in less uptake of positively charged U(VI) ions, because of electrostatic repulsion. At pH
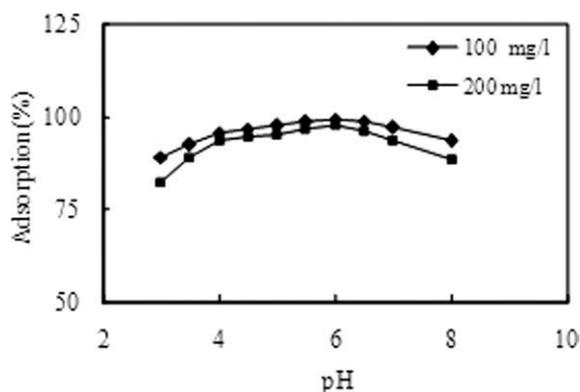
Figure 5 Effect of pH on U(VI) ions adsorption onto Cellu-*g*-PMAAc/Bent at temperature 30°C, equilibrium time 3 h, and the adsorbent dose 1 g/L.

Figure 6 Kinetic plots for the adsorption of U(VI) ions onto Cellu-*g*-PMAAc/Bent.

higher than 3.5 (4.0–6.0), carboxylic groups are deprotonated, and thus more available groups for ion exchange can be available. The ion exchange process is the major mechanism for the removal of U(VI) ions from solutions within this pH range. Thus, at pH 6.0, the Cellu-*g*-PMAAc/Bent could adsorb about 99.2% of U(VI) from an initial concentration of 100 mg/L, which is very high when compared with the earlier reported works, where the adsorption percentage was in the range 70.0%–90.0%.[26,27]

Kinetic study

The effect of contact time on the adsorption of U(VI) ions onto Cellu-*g*-PMAAc/Bent was studied in the concentration range 100–250 mg/L, and the results are shown in Figure 6. The equilibrium time was found to be 180 min. The adsorption is higher in the beginning because of greater number of reaction sites available for the adsorption of U(VI) ions. The initial concentration has no significant effect on the time to reach equilibrium. With the increase of initial U(VI) concentration from 100 to 250 mg/L, the adsorption capacity increases from 99.24 to 236.25 mg/g, indicating that U(VI) adsorption depends on the initial metal concentration. Adsorption kinetics of U(VI) ions onto Cellu-*g*-PMAAc/Bent was studied using pseudofirst-order and pseudosecond-order kinetic model.[28]
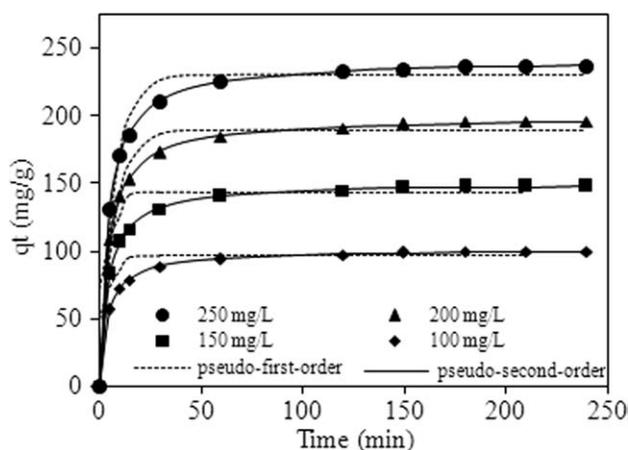
$$\text{pseudo-first-order} : q_t = q_e(1 - e^{-k_1 t}) \quad (5)$$

$$\text{pseudo-second-order} : q_t = \frac{k_2 q_e^2 t}{1 + k_2 q_e t}, \quad (6)$$

where q_e and q_t are the amounts of solute adsorbed per unit mass of the adsorbent at equilibrium and time t, respectively. k_1 and k_2 are the pseudofirst-order and pseudosecond-order rate constants, respectively. Parameters of the pseudofirst-order and pseudosecond-order kinetic models were estimated from the experimental data using nonlinear curve fitting procedure, and the results are presented in Table I.

To check the variation of both equations visually, the theoretical lines using these constants are also shown in Figure 6. The pseudofirst-order equation shows a poor correlation with experimental data, whereas the pseudosecond-order equation indicates a good correlation of the experimental results. Also, the values of R^2 and χ^2 listed in Table I reflect a better correlation for the pseudosecond-order model. In addition, q_e, which is the adsorption capacity, agreed very well with both the experimental and calculated values, as listed in Table I. The values of k_2 decrease with increasing metal concentration, which is consistent with studies reported before.[29,30] These results imply that chemisorption-like mechanism may play an important role for the adsorption of U(VI) ions onto Cellu-*g*-PMAAc/Bent.

TABLE I
Kinetic Parameters for the Adsorption of U(VI) Ions onto Cellu-*g*-PMAAc/Bent

	Pseudosecond-order					Pseudofirst-order			
Conc. (mg/L)	q_e exp. (mg/g)	k_2 (mg/g min)	q_e (mg/g)	χ^2	R^2	k_1 (/min)	q_e (mg/g)	χ^2	R^2
100	99.21	2.42×10^{-3}	100.82	0.39	0.999	0.142	96.21	20.17	0.979
150	147.33	1.60×10^{-3}	149.74	0.82	0.999	0.140	142.80	44.20	0.981
200	195.26	1.20×10^{-3}	198.16	1.84	0.999	0.138	188.92	79.73	0.979
250	236.25	0.91×10^{-3}	240.81	1.04	0.999	0.137	229.71	102.41	0.982

TABLE II
Diffusion Kinetic Parameters for the Adsorption of U(VI) Ions onto Cellu-*g*-PMAAc/Bent

Conc. (mg/L)	Diffusion coefficients	
	D_i (cm^2/s)	B_L (cm/s)
100	3.58×10^{-12}	1.66×10^{-4}
150	3.08×10^{-12}	1.25×10^{-4}
200	3.06×10^{-12}	1.05×10^{-4}
250	2.39×10^{-12}	0.74×10^{-4}

The equilibrium attainment may be due to mass transfer diffusion or intraparticle mass transfer diffusion. To assess the nature of the diffusion process responsible for adsorption of U(VI) on Cellu-*g*-PMAAc/Bent, the adsorption data were tested with the McKay equation for analyzing the external mass transfer diffusion and the Urano and Tachikawa equation for analyzing intraparticle mass transfer diffusion. The external mass transfer diffusion equation is generally expressed as follows[31]:

$$\ln\left[\left(\frac{C_t}{C_0}\right) - \frac{1}{(1+mK_L)}\right] = \ln\left[\frac{mK_L}{(1+mK_L)}\right] - \left[\frac{(1+mK_L)}{mK_L}\right]B_L S_S t, \quad (7)$$

where C_t is the concentration of the adsorbate at time t, C_0 is the initial concentration of the adsorbate, m is the mass of adsorbent per unit volume of particle-free adsorbate solution, K_L is the Langmuir constant (obtained by multiplying the Langmuir constants, Q^0 and b), S_s is the specific surface per unit volume of particle free slurry, and B_L is the mass transfer coefficient (cm/s). The values of B_L were calculated for different concentrations and listed in Table II. It can be shown that the B_L values decreases from 1.66×10^{-4} to 0.74×10^{-4} with increase in concentration from 100 to 250 mg/L. It can be attributed to the fact that increase in metal concentration in solution reduced the diffusion of metal ions in the boundary layers.

The intraparticle mass transfer diffusion equation is given as[32]:

$$f\left[\frac{q_t}{q_e}\right] = -\log\left[\left(\frac{q_t}{q_e}\right)^2\right] = \frac{4\pi^2 D_i t}{2.303 d^2}. \quad (8)$$
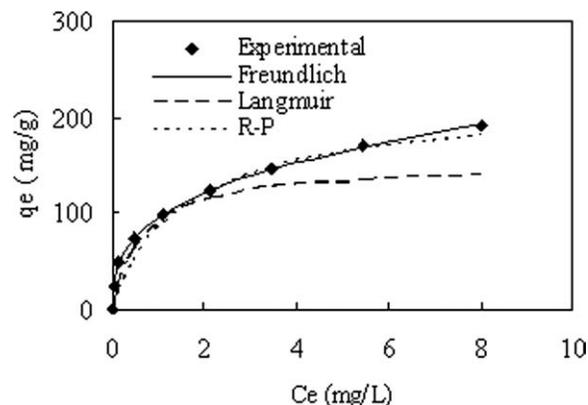

Figure 7 Comparison of different isotherm models to the experimental isotherm data for U(VI) ions adsorption onto Cellu-*g*-PMAAc/Bent.

In the equation cited above, q_t and q_e are the amount adsorbed at time t and at equilibrium respectively, d is the diameter of the adsorbent, and D_i is the intraparticle diffusion based on the concentration in solids (cm^2/s). The D_i values calculated are shown in Table II. The values showed that it decreases from 3.58×10^{-12} to 2.39×10^{-12} cm^2/s with increase in concentration from 100 to 250 mg/L. Increase in metal concentration may result in the decrease of intraparticle diffusion in the boundary layers. Earlier researchers[33] explained that the values of D_i in the range 10^{-12}–10^{-15} cm^2/s reflect intraparticle mass transfer diffusion process as the rate limiting step. The diffusion constants are of the order of 10^{-12} cm^2/s, which suggests that the rate limiting step appears to be intraparticle diffusion process.

Isotherm

The experimental data of equilibrium adsorption were analyzed using the nonlinear forms of Langmuir, Freundlich, and Redlich–Peterson isotherm equations.[34]

$$\text{The Langmuir adsorption isotherm}: q_e = Q^0 b C_e / 1 + bC_e \quad (9)$$

$$\text{The Freundlich adsorption isotherm}: q_e = K_F C_e^{1/n} \quad (10)$$

$$\text{The Redlich-Peterson isotherm}: q_e = \frac{K_k C_e}{a_R C_e} b + 1, \quad (11)$$

TABLE III
Isotherm Constants for the Adsorption of U(VI) Ions onto Cellu-*g*-PMAAc/Bent

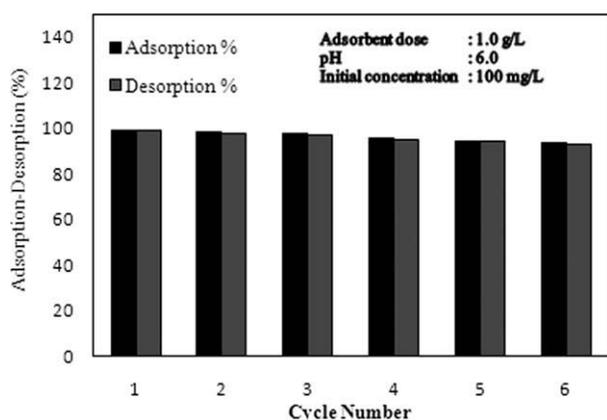| Langmuir				Freundlich				Redlich–Peterson				
Q^0 (mg/g)	B (mg/L)	R^2	χ^2	K_F	$1/n$	R^2	χ^2	K_R (mg/g)	B (mg/L)	a_R	R^2	χ^2
184.65	1.29	0.947	37.74	96.18	0.334	0.999	2.33	162.34	0.93	0.88	0.943	45.86

Figure 8 Adsorption/desorption cycles of U(VI) ions onto Cellu-*g*-PMAAc/Bent.

where q_e and C_e are the equilibrium concentrations of the U(VI) on the adsorbent and solution, respectively. $Q°$ and b are the Langmuir constants, K_F and $1/n$ are the Freundlich constants, and K_R, b, and a_R are the R–P constants. The experimental and model fit of q_e and C_e for the adsorption of U(VI) are shown in Figure 7. The values of isotherm constants were calculated using nonlinear regression analysis, and the results are listed in Table III. As can be seen from the results, equilibrium data agree well with the Freundlich model. The values of R^2 and χ^2 showed that the adsorption of U(VI) ions onto Cellu-*g*-PMAAc/Bent was best fitted with Freundlich isotherm model over the concentration ranges studied. Earlier study also showed that the adsorption of U(VI) ions is best fitted with Freundlich isotherm model.[35] The fact that the Freundlich isotherm fits the experimental data very well may be because of heterogenous distribution of active sites on the Cellu-*g*-PMAAc/Bent surface, since the Freundlich equation assumes that the surface is heterogeneous. The numerical value $0 < 1/n < 1.0$ obtained for the present system indicates favorable adsorption.

Reuse of the adsorbent

Desorption is an important process in adsorption studies, because it enhance the economical value of adsorption process. Desorption efficiency of the spent adsorbent was checked with HCl solution having different concentrations (0.001–0.1*M*). The desorption rises from 30.3% to a maximum value of 99.2% with increase in HCl concentration from 0.001 to 0.1*M*. The results demonstrated that the adsorbed U(VI) could be desorbed from the spent adsorbent using 0.1*M* HCl, and hence it was used to regenerate Cellu-*g*-PMAAc/Bent. The adsorption–desorption cycle was repeated six times with same adsorbent using 0.1*M* HCl. The results are shown in Figure 8.

Although there were slight reductions in the adsorption capacities with regeneration cycles, the spent adsorbent still possessed high adsorption capacity, and hence the adsorbent can be used successfully six times after regeneration for the removal and recovery of U(VI) from aqueous solutions.

CONCLUSIONS

In the present study, a novel adsorbent poly(methacrylic acid)-grafted-cellulose/bentonite (Cellu-*g*-PMAAc/Bent graft copolymer) was prepared, and its efficiency in removing U(VI) was tested by batch adsorption technique. The adsorbent was characterized by FTIR, SEM-EDS, and XRD analyses. The adsorption conditions for the adsorbent were optimized by varying several experimental parameters such as pH, contact time, and initial sorbate concentration of the solution. The U(VI) adsorption process, which was pH dependent, show maximum removal at pH 6.0. Adsorption equilibrium was achieved within 180 min. The adsorption data were modeled using pseudofirst-order and pseudosecond-order kinetic equations. Pseudosecond-order equation was well correlated with the experimental kinetic data. The Freundlich, Langmuir, and Redlich–Peterson isotherm model were used to describe the equilibrium data. Freundlich adsorption isotherm model gave good correlation with the experimental equilibrium data. Repeated adsorption–desorption study showed that Cellu-*g*-PMAAc/Bent graft copolymer can be effectively used as an adsorbent for the removal and recovery of U(VI) from aqueous solutions.

References

1. Xu, X. D.; Zhang, X. Z.; Cheng, S. X.; Zhuo, R. X.; Kennedy, J. F. Carbohydr Polym 2007, 68, 416.
2. Siddhanta, S. K.; Gangopadhyay, R. Polymer 2005, 46, 2993.
3. Pourjavadi, A.; Harzandi, A. M.; Amini-Fazl, M. S. Eur Polym Mater 2008, 44, 1209.
4. Liu, Z.; Luo, Y.; Zhang, K. J Biomater Sci Polymer 2008, 19, 1503.
5. Philippova, O. E.; Rulkens, R.; Kovtunenko, B. I.; Abramchuk, S. S.; Khokhlov, A.; Wegner, G. Macromolecules 1998, 31, 1168.
6. Ekine, S.; Istkver, F.; Saraydin, D. Polym Bull 2006, 57, 231.
7. Kundakci, S.; Uzum, O. B.; Karadag, E. React Funct Polym 2008, 68, 458.
8. Ulusoy, U.; Simsek, S.; Ceyhan, O. Adsorption 2003, 9, 165.
9. Chisholm-Brause, C. J.; Berg, J. M.; Matzner, R. A.; Morris, D. E. J Colloid Interface Sci 2001, 233, 38.
10. Aycik, G. A.; Gurellier, R. J Radioanal Nucl Chem 2007, 273, 713.

11. Li, X.; Xu, S.; Wang, J.; Chen, X.; Fens, S. Carbohydr Polym 2009, 75, 688.
12. Liu, J.; Wang, X.; Xu, T.; Shao, G. Sep Purif Technol 2009, 66, 135.
13. Nishimura, M.; Higa, M.; Akamine, K.; Masudaya, S. Desalination 2008, 233, 157.
14. Rump, H. H.; Krist, H. Laboratory Manual for the Examination of Water, Waste Water and Soil; VCH publications: Weinheim, 1992.
15. Magdy, K. Z. J Polym Res 2006, 13, 65.
16. Nakanishi, K. Infrared Absorption Spectroscopy; Holden-Day Inc. and Nankodo Company Limited, Tokyo, 1962.
17. Zazhogin, A. P.; Komyak, A. I.; Umreiko, D. S. J Appl Spectrosc 2008, 75, 735.
18. Zhao, H.; Kwak, J. H.; Zhang, Z. C.; Brown, H. M.; Arey, B. W.; Holladay, J. E. Carbohydr Polym 2007, 68, 235.
19. Inoue, K.; Kawakita, H.; Ohto, K.; Oshima, T.; Murakami, H. J Radioanal Nucl Chem 2006, 267, 435.
20. Zhang, J.; Yuan, K.; Wang, Y. P.; Gu, S. J.; Zhang, S. Mater Lett 2007, 61, 316.
21. An, L.; Aiqin, W. Eur Polym Mater 2005, 41, 1630.
22. Flory, P. J. Principles of Polymer Chemistry; Cornell University Press: Ithaca, NY, 1953.
23. Peppas, L. B.; Harlamd, R. S. Absorbent Polymer Technology; Elsevier: Amsterdam, 1990.
24. Volker, S.; Rieckmann, T. J Anal Appl Pyrolysis 2002, 62, 165.
25. Wan, T.; Wang, X.; Yuan, Y.; He, W. Polym Int 2006, 55, 1413.
26. Zhiweia, N.; Qiaohuia, F.; Wenhuaa, W.; Junzhenga, X.; Leib, C.; Wangsuo, W. Appl Radiat Isotopes 2009, 67, 1582.
27. Nathalie, C.; Richard, G.; Eric, D. Water Res 2003, 37, 3079.
28. Anirudhan, T. S.; Radhakrishnan, P. G. J Colloid Interface Sci 2007, 316, 268.
29. Anoop Krishnan, K.; Anirudhan, T. S. J Hazard Mater B 2002, 92, 161.
30. Ho, Y. S. Adsorption 2004, 10, 151.
31. Mckay, G.; Otterburn, M. S.; Sweeny, A. J Water Res 1981, 15, 327.
32. Urano, K.; Tachikawa, H. Ind Eng Chem Res 1991, 30, 1897.
33. Vinod, V. P.; Anirudhan, T. S. J Chem Technol Biotechnol 2001, 77, 92.
34. Tsai, W. T.; Hsu, H. C.; Su, T. Y.; Lin, K. Y.; Lin, C. M. J Colloid Interface Sci 2006, 299, 513.
35. Donat, R.; Aytas, S. J Radioanal Nucl Chem 2005, 265, 107.